

Dark matter and sub-GeV hidden $U(1)$ in GMSB models

Eung Jin Chun* and Jong-Chul Park†

Korea Institute for Advanced Study, Heogiro 87, Dongdaemun-gu, Seoul 130-722, Korea

ABSTRACT: Motivated by the recent PAMELA and ATIC data, one is led to a scenario with heavy vector-like dark matter in association with a hidden $U(1)_X$ sector below GeV scale. Realizing this idea in the context of gauge mediated supersymmetry breaking (GMSB), a heavy scalar component charged under $U(1)_X$ is found to be a good dark matter candidate which can be searched for direct scattering mediated by the Higgs boson and/or by the hidden gauge boson. The latter turns out to put a stringent bound on the kinetic mixing parameter between $U(1)_X$ and $U(1)_Y$: $\theta \lesssim 10^{-6}$. For the typical range of model parameters, we find that the decay rates of the ordinary lightest neutralino into hidden gauge boson/gaugino and photon/gravitino are comparable, and the former decay mode leaves displaced vertices of lepton pairs and missing energy with distinctive length scale larger than 20 cm for invariant lepton pair mass below 0.5 GeV. An unsatisfactory aspect of our model is that the Sommerfeld effect cannot raise the galactic dark matter annihilation by more than 60 times for the dark matter mass below TeV.

KEYWORDS: dark matter, cosmic rays, cosmology of theories beyond the SM.

*ejchun@kias.re.kr

†jcpark@kias.re.kr

Contents

1. Introduction	1
2. Spontaneous breaking of hidden $U(1)_X$ by gauge mediation	3
3. Kinetic mixing between gauge bosons/gauginos of $SU(2)_L \times U(1)_Y$ and a hidden $U(1)_X$	5
4. Relic density, positron/electron excess and direct detection	6
5. Visible OLSP decay and Displaced vertices of lepton pairs	10
6. Conclusion	12

1. Introduction

It is now firmly established that 23% of the energy density of the universe consists of an unknown particle called dark matter. Discovering the nature of dark matter would be one of the most important tasks in current and future theoretical and experimental investigations. Numerous searches for galactic dark matter have been made to observe direct signals of dark matter scattering with nuclei and indirect evidences of dark matter annihilation to various Standard Model particles. Recently, a number of stimulating results toward indirect signals have been announced.

The Payload for Antimatter Matter Exploration and Light-nuclei Astrophysics (PAMELA) collaboration has reported an excess in the positron fraction, $e^+/(e^+ + e^-)$, but no excess in anti-proton fraction \bar{p}/p [1]. The observed spectrum departed from the background calculation of the cosmic-ray secondary positron spectrum [2] for energies 10–100 GeV. This recent result is comparable with less certain excesses observed in HEAT [3] and AMS-01 [4]. The PPB-BETS balloon experiment and the Advanced Thin Ionization Calorimeter (ATIC) instrument have also reported an excess in the $e^+ + e^-$ energy spectrum of 300 – 800 GeV [5, 6].

The origin of such excesses could be astronomical objects such as a pulsar which is expected to emit energetic electron-positron pairs [7, 8, 9]. On the other hand, excessive antiparticle fluxes in galactic cosmic rays have been considered as a primary way for indirect detection of dark matter. It is encouraging that galactic dark matter annihilation can easily reproduce the amplitudes and spectral shapes of the PAMELA

and ATIC data. However, there appear two puzzling aspects. First, the dark matter annihilation cross-section is required to be enhanced by order of $100 - 1000$ compared with what is allowed by the standard thermal relic abundance analysis. According to a recent analysis based on Λ CDM N -body simulations, however, the boost factor from clumpy matter distribution can hardly larger than about 10 [10]. Second, no distinctive excess of antiprotons in the PAMELA data disfavors most conventional dark matter candidates. A new analysis of the \bar{p}/p ratio compared to the PAMELA data puts stringent limits on possible enhancements of the \bar{p}/p flux from dark matter annihilation [11]. Many ideas and models of dark matter annihilation or decay have already been suggested for the explanation of the recent observations [12, 13, 14, 15, 16, 17, 18, 19, 20, 21, 22, 23, 24, 25, 26, 27, 28, 29, 30, 31, 32, 33, 34, 35, 36, 37]. However, it appears to be a hard task to understand the nature of enhanced hadrophobic annihilation in a consistent framework with thermal dark matter.

In this paper, we elaborate the idea of dark matter charged under an extra $U(1)_X$ gauge group suggested in Refs. [20, 38, 39]. The presence of $U(1)_X$ broken at the sub-GeV scale is motivated to explain the two intriguing features of the PAMELA data. First, the DM annihilation to extra light gauge bosons can be enhanced significantly by non-perturbative Sommerfeld effect [40, 41, 42, 43, 44]. Second, the hadrophobic nature of the $U(1)_X$ gauge boson decay can be understood by kinematics when its mass is below the GeV scale [20, 24]. We will consider the extra $U(1)_X$ gauge boson hidden from the Standard Model sector except for a small kinetic mixing between $U(1)_X$ and $U(1)_Y$, through which the $U(1)_X$ gauge bosons can decay mostly into lepton-antileptons. It was shown long ago that kinetic mixing can exist between two $U(1)$ gauge bosons without violating the gauge-invariance and renormalizability [45]. The mixing between an unbroken extra $U(1)$ and $U(1)_{em}$ has been used to explain other anomalous astronomical observation such as galactic 511 keV γ -rays [46].

Breaking $U(1)_X$ below the GeV scale can arise naturally by radiative mechanism, in particular, in the context of gauge mediated supersymmetry breaking (GMSB) [39]. We will first present a concrete way of realizing such a scheme, which predicts a $U(1)_X$ charged scalar field as a dark matter candidate. The dark matter mass in the range of 600–1000 GeV is preferred for the simultaneous explanation of the PAMELA and ATIC data. Unfortunately, the Sommerfeld enhancement factor of our scenario is found to be about 40–60 for this mass range. The assumption of some clumpy distribution of dark matter would be a reasonable additional source for further increase of the boost factor. Our dark matter candidate can yield observable signals for direct detection through elastic scatterings mediated by the hidden gauge boson X or Higgs bosons. In the first case, we draw a severe constraint on the kinetic mixing parameter: $\theta \lesssim 10^{-6}$ for $m_X \sim 0.4$ GeV. One of the interesting consequences of our scenario is that the ordinary lightest supersymmetric particle (OLSP), typically neutralino, decays instantaneously to the X boson and its superpartner \tilde{X} through

one-loop diagram with heavy dark matter superfields in the loop. Then, the produced X boson subsequently decays to two leptons with a decay length typically larger than 10 cm, which may be observed at the LHC.

2. Spontaneous breaking of hidden $U(1)_X$ by gauge mediation

Let us start with working in gauge mediated supersymmetry breaking (GMSB) models [47] as a promising way of realizing the sub-GeV $U(1)_X$ sector. In such a scheme, the origin of a heavy mass of dark matter from the hidden $U(1)_X$ sector and the μ term can be related in the context of non-minimal supersymmetric standard model [39]:

$$W = \frac{\lambda_S}{3} S^3 + \lambda_q S q' q'^c + \lambda_H S H_1 H_2 + \lambda_\Psi S \Psi \Psi^c, \quad (2.1)$$

where (Ψ, Ψ^c) is the Dirac pair carrying $U(1)_X$ charge $(+1, -1)$. Note that the second term with extra quark pairs is introduced to generate sufficiently large negative mass-squared for S and thus a large vacuum expectation value v_S , which will lead to proper electroweak symmetry breaking [48]. A similar mechanism will be used to break $U(1)_X$ at the sub-GeV scale in the below. Having generated v_S , one obtains μ and B terms for the Higgs fields: $\mu = \lambda_H v_S$ and $B = \lambda_S v_S$. Similarly, we also obtain the supersymmetric mass of hidden Dirac fermions $m_\psi \equiv \lambda_\Psi v_S$ and the corresponding (Dirac) soft bilinear term:

$$V_{soft} = B m_\psi \tilde{\psi} \tilde{\psi}^c + h.c.. \quad (2.2)$$

Because of this mixing mass term, two hidden scalars $\tilde{\psi}$ and $\tilde{\psi}^c$ have mass splitting and the mass eigenstates denoted by $\tilde{\psi}_{1,2}$ have the masses $m_{\tilde{\psi}_{1,2}}$ where $m_{\tilde{\psi}_{1,2}}^2 = m_\psi^2 \mp B m_\psi$ taking B is real positive. Therefore, the lighter scalar $\tilde{\psi}_1$, being lighter than the Dirac fermion (ψ, ψ^c) , will be our dark matter particle.

Let us turn to supersymmetry breaking fed into the hidden $U(1)_X$ sector. Note that the Dirac superfield (Ψ, Ψ^c) plays a role of ‘messenger field’ for the hidden sector supersymmetry breaking whose size is controlled by the B parameter. That is, the supersymmetry breaking masses of the hidden gaugino \tilde{X} and the scalar component ϕ_x of a hidden superfield Φ_x , carrying $U(1)_X$ charge x , are given by

$$\begin{aligned} m_{\tilde{X}} &= \frac{\alpha_X}{4\pi} B \\ m_{\phi_x}^2 &= 2x^2 m_{\tilde{X}}^2 \end{aligned} \quad (2.3)$$

which are defined at the ‘messenger scale’ m_ψ . Here $\alpha_X = g_X^2/4\pi$ is the $U(1)_X$ gauge fine structure constant. The reference value for the hidden gaugino mass is $m_{\tilde{X}} \approx 0.3$ GeV for $\alpha_X = \alpha$ and $B = 500$ GeV. Consider now the following hidden sector superpotential:

$$W = \lambda_1 \Phi_0 \Phi_z \Phi_{-z} + \lambda_p \Phi_0 \Phi_{pz} \Phi_{-pz} + \frac{\lambda_0}{3} \Phi_0^3, \quad (2.4)$$

where the subscripts denote the $U(1)_X$ charges. Denoting m_x as the soft mass of the scalar component ϕ_x , we get $m_{pz}^2 = p^2 m_z^2$ and $m_0^2 = 0$ at the messenger scale m_ψ . Then, one can generate a large negative mass-squared for ϕ_0 down around the scale m_{pz} assuming $m_{pz}^2 \gg m_z^2$ ($p > 1$) and the Yukawa coupling λ_p of order one:

$$m_0^2 \approx -n \frac{p^2 \lambda_p^2}{4\pi^2} m_z^2 \ln \frac{m_\psi}{pm_z}, \quad (2.5)$$

where n is the number of the $\Phi_{\pm pz}$ pairs. This will induce a sizable mixing vacuum expectation value v_0 of ϕ_0 determined to be $v_0^2 = -m_0^2/2\lambda_0^2$. Then the scalar potential for $\phi_{\pm z}$ is given by

$$V = \lambda_1^2 |\phi_z \phi_{-z}|^2 + [\lambda_1 \lambda_0 v_0^2 \phi_z \phi_{-z} + c.c.] + (\lambda_1^2 v_0^2 + m_z^2)[|\phi_z|^2 + |\phi_{-z}|^2]. \quad (2.6)$$

If the mixing mass term of $\phi_z \phi_{-z}$ is larger than the diagonal mass $m_z^2 + \lambda_1^2 v_0^2$, there appears a direction of negative mass-squared and thus $U(1)_X$ symmetry breaking occurs. For the minimization of the above potential, we examine the D-flat direction $\phi_{-z} = \phi_z$ which has the mass eigenvalues $m_\pm^2 = 2(m_z^2 + \lambda_1^2 v_0^2 \pm \lambda_1 \lambda_0 v_0^2)$. To get $m_-^2 < 0$ and thus $v_z^2 \equiv \langle \phi_z \rangle^2 = -m_0^2/\lambda_1^2$, one needs to have

$$-m_0^2 > 8m_z^2 \quad (2.7)$$

assuming $\lambda_0 = 2\lambda_1 < \lambda_p \sim 1$. This condition can be generically met by adjusting the parameters n, p in Eq. (2.5). Given v_z , the X gauge boson gets the mass

$$m_X = 2g_X z v_z. \quad (2.8)$$

The X boson mass is therefore settled down around the hidden gaugino mass scale $m_{\tilde{X}}$. However, their specific values will depend on the choice of the parameters n, p and the couplings $\lambda_{0,1,p}$.

Note that the hidden $U(1)_X$ sector can have a communication with the Standard Model sector through the Yukawa couplings, λ_H and λ_Ψ . In particular, our scalar dark matter $\tilde{\psi}_1$ can annihilate to quarks and leptons through the Higgs contact interaction:

$$\mathcal{L} = -\frac{1}{2} \lambda_H \lambda_\Psi H_1 H_2 \tilde{\psi}_1 \tilde{\psi}_1^* + h.c.. \quad (2.9)$$

We want this channel to be subdominant to the dark matter annihilation into the light hidden fields as alluded in the introduction. For this purpose, we will assume

$$\lambda_H \lambda_\Psi \ll g_X^2 \quad (2.10)$$

throughout this paper. Then, there can also be kinetic mixing between $U(1)_X$ and $U(1)_Y$ through which the X gauge boson can decay to leptons as will be discussed in the next section. The interaction (2.9) will give an important contribution to dark

matter scattering off nuclei through the Higgs exchange. In the decoupling limit of heavy neutral Higgs, the interaction between $\tilde{\psi}_1$ and the light Higgs h^0 is given by

$$\mathcal{L} = \lambda v h^0 \tilde{\psi}_1 \tilde{\psi}_1^*, \quad (2.11)$$

where $\lambda \equiv s_\beta c_\beta \lambda_H \lambda_\Psi / 2$. Here $\langle H_{1,2}^0 \rangle = v_{1,2} / \sqrt{2}$ and $\tan \beta \equiv v_2 / v_1$.

3. Kinetic mixing between gauge bosons/gauginos of $SU(2)_L \times U(1)_Y$ and a hidden $U(1)_X$

If $U(1)_X$ was unbroken, it mixes with $U(1)_{em}$ and various interesting phenomena of milli-charged dark matter particles can occur [See [46] and references therein, and see [49] and references therein for the Stueckelberg extension with kinetic mixing]. When $U(1)_X$ is broken, the massive X gauge boson mixes essentially with the Z boson and leads to phenomenological consequences drastically different from the previous case. Consider the gauge kinetic terms of $SU(2)_L \times U(1)_Y \times U(1)_X$ including the kinetic mixing term:

$$\mathcal{L}_{\text{mixing}} = -\frac{\sin \theta}{2} \hat{B}^{\mu\nu} \hat{X}_{\mu\nu}. \quad (3.1)$$

The canonical form of the gauge kinetic term can be made by the following transformation:

$$\begin{pmatrix} \hat{B}_\mu \\ \hat{X}_\mu \end{pmatrix} = \begin{pmatrix} \sec \theta & 0 \\ -\tan \theta & 1 \end{pmatrix} \begin{pmatrix} B'_\mu \\ X'_\mu \end{pmatrix}. \quad (3.2)$$

After the $SU(2)_L \times U(1)_Y \times U(1)_X$ breaking, the canonical gauge fields get masses and mixing. Diagonalizing the gauge boson mass matrix, one finds the relation between the original gauge eigenstates \hat{W}^3 , \hat{B} , and \hat{X} and mass eigenstates Z , A , and X :

$$\begin{pmatrix} \hat{W}_\mu^3 \\ \hat{B}_\mu \\ \hat{X}_\mu \end{pmatrix} = \begin{pmatrix} c_W & s_W & -\frac{c_W s_W m_Z^2}{m_Z^2 - m_X^2} \theta \\ -s_W & c_W & -\frac{c_W^2 m_Z^2 - m_X^2}{m_Z^2 - m_X^2} \theta \\ \frac{s_W m_Z^2}{m_Z^2 - m_X^2} \theta & 0 & 1 \end{pmatrix} \begin{pmatrix} Z_\mu \\ A_\mu \\ X_\mu \end{pmatrix} + \mathcal{O}(\theta^2). \quad (3.3)$$

Let us now present some couplings relevant for our discussions in the limit of $\theta \ll 1$ and $m_X \ll m_Z$. The scalar dark matter $\tilde{\psi}_1$ has the gauge interactions with X and Z as follows:

$$\mathcal{L} = ig_X (\tilde{\psi}_1^* \partial^\mu \tilde{\psi}_1 - \partial^\mu \tilde{\psi}_1^* \tilde{\psi}_1) (X_\mu + \theta s_W Z_\mu) + g_X^2 \tilde{\psi}_1^* \tilde{\psi}_1 X^\mu X_\mu. \quad (3.4)$$

The hidden gauge boson X couples also to the visible sector particles, which is described by

$$\mathcal{L} = \theta g' X_\mu \bar{f} \gamma^\mu \Gamma_{fX} f \quad (3.5)$$

$$\text{with } \Gamma_{fX} \approx -Q_f c_W^2 \text{ and } \Gamma_{\nu X} = -\frac{m_X^2}{2m_Z^2} P_L,$$

where Q_f is the electromagnetic charge of a quark or lepton and again the sub-leading terms of order of m_X^2/m_Z^2 are neglected except for neutrinos. In addition, the coupling of XWW , g_{XWW} , is given by $g_{XWW} = -\theta s_W g_{ZWW}$ where g_{ZWW} is the SM coupling of ZWW .

The supersymmetric counterpart of Eq. (3.2) can be read straightforwardly [50], that is, the original hidden gaugino can be replaced by the relation,

$$\hat{X} = \tilde{X} - \theta \tilde{B} \quad (3.6)$$

leading to the bino interaction to the hidden sector fermion and scalar. In the right-hand side of the above equation, the gauginos can be considered as the mass eigenstates as the mixing mass $\theta m_{\tilde{X}}$ between \tilde{X} and \tilde{B} arising from the previous consideration can be safely neglected in our discussion. The coupling of bino to light hidden sector bosons and fermions given by

$$\mathcal{L} = \theta g_X \tilde{B} \tilde{\phi} \phi^* + h.c. \quad (3.7)$$

provides a decay channel of the ordinary lightest supersymmetric particle in the visible sector.

4. Relic density, positron/electron excess and direct detection

With the assumption of Eq. (2.10) and $\theta \ll 1$, which will be discussed shortly, we can neglect the dark matter annihilation to the Standard Model particles through Higgs and Z, X gauge boson channels, namely, $\tilde{\psi}_1 \tilde{\psi}_1^* \rightarrow HH, XZ$ and ZZ . Then, the dark matter relic density is determined by the process $\tilde{\psi}_1 \tilde{\psi}_1^* \rightarrow XX$ having the cross-section:

$$\langle \sigma v \rangle_{XX} \simeq \frac{4\pi \alpha_X^2}{m_{\tilde{\psi}_1}^2}. \quad (4.1)$$

The present relic density of $\tilde{\psi}_1$ is then given by

$$\begin{aligned} \Omega_{\tilde{\psi}_1} h^2 &\simeq \frac{1.07 \times 10^9 \text{ GeV}^{-1} x_F}{M_{pl}} \frac{1}{\sqrt{g_*} \langle \sigma v \rangle_{XX}} \\ &\approx \frac{2.17 \times 10^{-10} \text{ GeV}^{-2}}{\langle \sigma v \rangle_{XX}}, \end{aligned} \quad (4.2)$$

where g_* counts the number of relativistic degrees of freedom and $x_F \equiv m/T_F$ [51]. The observed value of $\Omega_{\text{DM}} h^2 \simeq 0.1143$ [52] fixes the hidden gauge coupling constant in terms of the dark matter mass:

$$\alpha_X \simeq 1.58 \alpha \left(\frac{m_{\tilde{\psi}_1}}{\text{TeV}} \right). \quad (4.3)$$

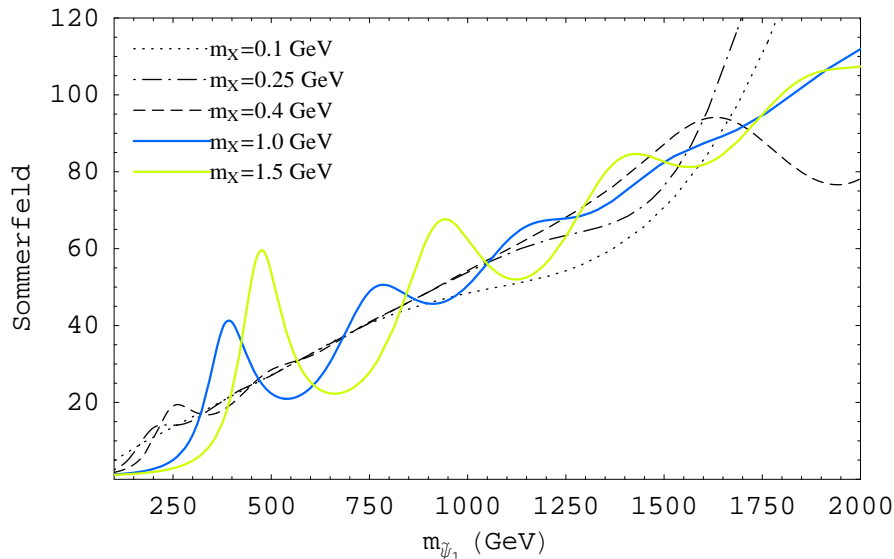


Figure 1: The Sommerfeld enhancement factor S as a function of $m_{\tilde{\psi}_1}$ for various m_X .

One of the troubles for the thermal dark matter explaining the recent positron/electron excesses from the galactic dark matter annihilation is the big gap between the cross section $\langle\sigma v\rangle_{\text{GAL}}$ required by the PAMELA and ATIC results and the cross section $\langle\sigma v\rangle_{\text{F.O.}}$ required by the dark matter relic density at the epoch of freeze-out. Their ratio is shown to be

$$\frac{\langle\sigma v\rangle_{\text{GAL}}}{\langle\sigma v\rangle_{\text{F.O.}}} \sim 10^{2-3} \left(\frac{M}{\text{TeV}}\right)^2 = B_e S, \quad (4.4)$$

where B_e is the boost factor for the positron/electron and S is the Sommerfeld enhancement factor [18]. In our model, the Sommerfeld enhancement arises due to the light gauge boson, and is calculated as $S = |\tilde{\psi}_1(\infty)/\tilde{\psi}_1(0)|^2$ after solving the following equation:

$$-\frac{1}{m_{\tilde{\psi}_1}} \frac{d^2 \tilde{\psi}_1(r)}{dr^2} - \frac{\alpha_X}{r} e^{-m_X r} \tilde{\psi}_1(r) = m_{\tilde{\psi}_1} \beta^2 \tilde{\psi}_1(r) \quad (4.5)$$

with the out-going boundary condition, $\tilde{\psi}'_1(\infty)/\tilde{\psi}_1(\infty) = im_{\tilde{\psi}_1}\beta$ where β is the dark matter velocity [18, 20, 41, 42, 43, 44]. Requiring the relic density condition (4.3), the Sommerfeld factor becomes a function of two input parameters, $m_{\tilde{\psi}_1}$ and m_X , which is shown in Fig. 1. As can be seen, the Sommerfeld enhancement factor is around 50 for $m_{\tilde{\psi}_1} \sim 800$ GeV, and increases almost linearly as $m_{\tilde{\psi}_1}$ increases except resonance effect for certain values. Our enhancement factor turns out to be insufficient to explain the PAMELA/ATIC data. This may indicate the presence of the combined effect with the boost factor $\lesssim 10$ from clumpy dark matter distribution [10].

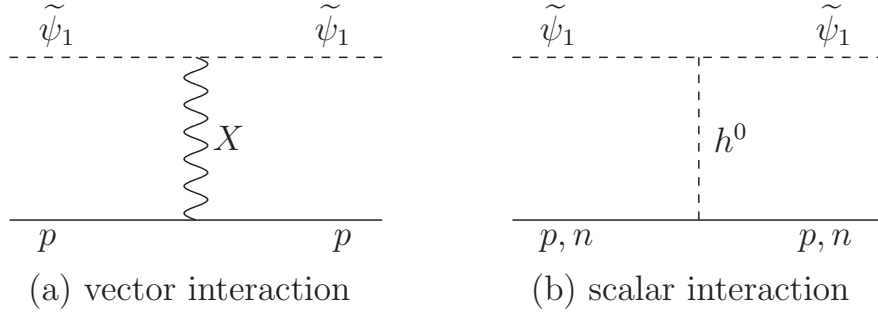


Figure 2: Diagrams relevant to $\tilde{\psi}_1$ -nucleon elastic scattering.

Given the interactions (2.11,3.4,3.5) of the hidden matter to the visible particles, some of our parameter space is constrained by dark matter experiments for direct detection. First, the dark matter $\tilde{\psi}_1$ has the effective vector interactions with quarks due to their couplings to the X gauge boson:

$$\mathcal{L}_{\text{vector}}^q = b_q i (\partial^\mu \tilde{\psi}_1^* \tilde{\psi}_1 - \tilde{\psi}_1^* \partial^\mu \tilde{\psi}_1) \bar{q} \gamma^\mu q, \quad (4.6)$$

where $b_q \equiv \theta g_X g' c_W^2 Q_q / m_X^2$. Now that the vector current is conserved, the contributions of each quark in a nucleus add coherently. In addition, sea quarks and gluons cannot contribute to the vector current. Thus, the $\tilde{\psi}_1$ -proton/neutron interactions can be expressed with the replaced couplings, $b_p = 2b_u + b_d$ and $b_n = b_u + 2b_d$. Note that we have $b_n \approx 0$ as X couples to the electromagnetic charge in the leading order. As a result, the $\tilde{\psi}_1$ -nucleus interaction is given by

$$\mathcal{L}_{\text{vector}}^N = b_N i (\partial^\mu \tilde{\psi}_1^* \tilde{\psi}_1 - \tilde{\psi}_1^* \partial^\mu \tilde{\psi}_1) \bar{N} \gamma^\mu N, \quad (4.7)$$

where $b_N = Z b_p + (A - Z) b_n = \theta g_X g' c_W^2 Z / m_X^2$ and the nucleus N has the atomic number Z and the atomic weight A . Therefore, the standard total cross section for the $\tilde{\psi}_1$ -nucleus vector interaction is given by [53]

$$\begin{aligned} \sigma_{\text{vector}}^{\tilde{\psi}_1-N} &= \frac{m_{\tilde{\psi}_1}^2 m_N^2 b_N^2}{64\pi (m_{\tilde{\psi}_1} + m_N)^2} \\ &\simeq 1.25 \times 10^4 \frac{\bar{m}_{\tilde{\psi}_1}^2 \bar{m}_N^2}{(\bar{m}_{\tilde{\psi}_1} + \bar{m}_N)^2} \theta^2 \frac{\alpha_X}{\alpha} \frac{Z^2}{\bar{m}_X^4} \text{ pb}, \end{aligned} \quad (4.8)$$

where $\bar{m}_i \equiv m_i / \text{GeV}$. Recall that the vector interaction leads only to spin-independent cross-section. To compare with experiments, we plot the $\tilde{\psi}_1$ -proton cross section for vector interactions given by

$$\sigma_{\text{vector}}^{\tilde{\psi}_1-p} = \sigma_{\text{vector}}^{\tilde{\psi}_1-N} \frac{1}{Z^2} \frac{\mu_p^2}{\mu_N^2}, \quad (4.9)$$

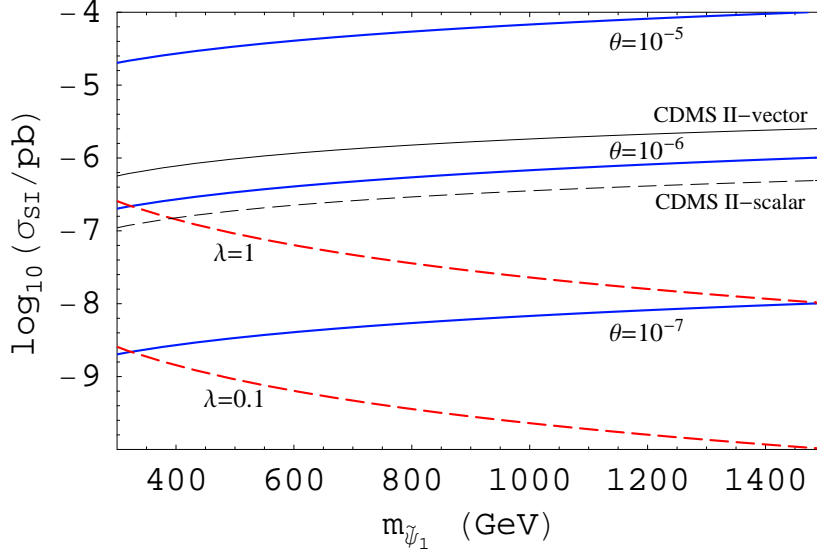


Figure 3: Exclusion plot for the spin-independent $\tilde{\psi}_1$ -nucleon cross-section σ_{SI} . The solid lines are the cross-sections via vector interactions with $m_X = 0.4$ GeV corresponding to $\theta = 10^{-5}, 10^{-6}$, and 10^{-7} , respectively. The dashed lines are through Higgs exchange corresponding to $\lambda = 1$ and 0.1 , respectively, taking $m_h = 115$ GeV. The thin solid (dashed) line shows the CDMS II limit for the vector (scalar) interaction.

where $\mu_{p,N}$ are the reduced masses for the $\tilde{\psi}_1$ -proton and $\tilde{\psi}_1$ -nucleus.

In addition to the vector interaction, the scalar dark matter $\tilde{\psi}_1$ interacts with nucleons through t -channel Higgs exchange driven by Eq. (2.11). The $\tilde{\psi}_1$ -nucleon cross section for the scalar interaction is adequately estimated in [54]:

$$\begin{aligned} \sigma_{\text{scalar}}^{\tilde{\psi}_1-n,p} &\approx \left(\frac{\lambda \, 0.34 \text{ GeV}}{m_h^2 \pi} \right)^2 \left(\frac{m_p}{m_{\tilde{\psi}_1} + m_p} \right)^2 \\ &\simeq 4.56 \times 10^6 \frac{\lambda^2}{\bar{m}_h^4} \frac{\bar{m}_p^2}{(\bar{m}_{\tilde{\psi}_1} + \bar{m}_p)^2} \text{ pb} , \end{aligned} \quad (4.10)$$

where $\bar{m}_i \equiv m_i/\text{GeV}$. If the Standard Model Higgs and hidden light higgs have the contact interaction term, $\lambda_{\phi h} \phi^2 h^2$, the hidden higgs mixes with the SM Higgs when both fields have vacuum expectation values. Therefore, the t -channel exchange of the light hidden scalar through this mixing possibly dominates in some cases [55]. However, in our model, the visible and hidden sectors are separated, and so no such contact interaction exists at the tree-level. The t -channel light scalar exchange can effectively arise only from three-loop diagrams, which can be safely neglected.

The Korea Invisible Mass Search (KIMS) experiment provides the most stringent limit on the spin-dependent interaction for a pure proton case [56], and the Cryogenic Dark Matter Search (CDMS II) experiment sets the strongest limit on the

spin-independent WIMP-nucleon interaction for a WIMP mass larger than ~ 100 GeV [57]. However, the latter is only relevant in this analysis. In Fig. 3, we present the $\tilde{\psi}_1$ -nucleon cross-sections via vector interactions (solid lines) as a function of $m_{\tilde{\psi}_1}$ for typical kinetic mixing parameters, $\theta = 10^{-5}, 10^{-6}$, and 10^{-7} . The scalar interaction cross-sections (dashed lines) are also shown as a function of $m_{\tilde{\psi}_1}$ for $\lambda = 1$ and 0.1 . The limits from CDMS II experiment is shown as thin line respectively for the vector and scalar interaction. The vector interaction puts a strong bound on the kinetic mixing parameter:

$$\theta \leq 2 \times 10^{-6} \left(\frac{m_X}{0.4 \text{ GeV}} \right)^2, \quad (4.11)$$

whereas the scalar interaction puts almost no bound on $\lambda = s_\beta c_\beta \lambda_H \lambda_\Psi / 2$. We remark that in the framework of the *inelastic dark matter* [58] one can evade this stringent bound on the kinetic mixing parameter θ as discussed in [20], where the dark matter is part of a multiplet of a non-Abelian gauge group and small mass splittings exist between these states. In this case, the most stringent bound on kinetic mixing comes from the anomalous magnetic moment of muon: $\theta \lesssim 9 \times 10^{-3} (m_X / 0.4 \text{ GeV})$ [59].

5. Visible OLSF decay and Displaced vertices of lepton pairs

In our scenario, the ordinary lightest supersymmetric particle (OLSP) χ_1^0 , which is typically a linear combination of neutralinos including singlino \tilde{S} , can decay to the hidden sector particles either through the kinetic mixing (3.7) or through the singlino coupling to the dark matter superfield components $\psi, \tilde{\psi}$ (2.1). The latter leads to the OLSF decay into hidden gauge boson X and gaugino \tilde{X} resulting from the one-loop induced $\tilde{S} - X - \tilde{X}$ interaction as shown in Fig. 4. The corresponding effective Lagrangian is

$$\mathcal{L} = \frac{1}{2} (C_1 + C_2) \tilde{X} \sigma^{\mu\nu} \tilde{S} X_{\mu\nu} \quad (5.1)$$

with $C_i = \frac{m_\psi}{16\pi^2 m_i^2} \frac{\lambda_\Psi g_X^2}{\sqrt{2}} J(x_i),$

where $x_i = m_\psi^2 / m_i^2$, $m_{1,2}^2 \equiv m_{\tilde{\psi}_{1,2}}^2 = m_\psi^2 \mp Bm_\psi$, and $J(x) \equiv \frac{1}{(1-x)^3} [-2 + 2x - (1+x) \ln x]$. In the limit of $x \rightarrow 1$, we have $J(x) = 1/6$ and the decay rate of the singlino \tilde{S} becomes

$$\Gamma(\tilde{S} \rightarrow X\tilde{X}) = \frac{1}{8\pi} m_{\tilde{S}}^3 (C_1 + C_2)^2 \approx \frac{\lambda_\Psi^2 \alpha_X^2}{2304\pi^3} \frac{m_{\tilde{S}}^3}{m_\psi^2}, \quad (5.2)$$

if the singlino is the OLSF. In the case of the bino OLSF, the decay rate of the bino \tilde{B} to hidden higgs and higgsinos (ϕ and $\tilde{\phi}$) via the kinetic mixing is given by

$$\Gamma(\tilde{B} \rightarrow \phi\tilde{\phi}) \approx \frac{\alpha_X \theta^2}{2} m_{\tilde{B}}. \quad (5.3)$$

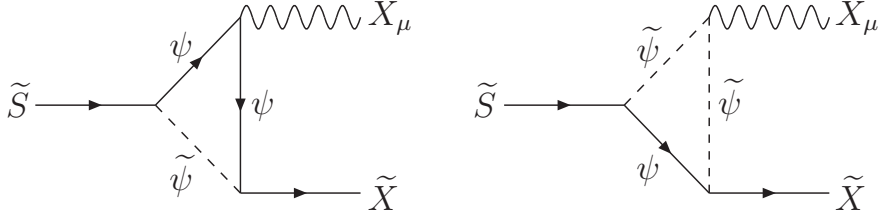


Figure 4: One-loop diagrams responsible for the decay of singlino \tilde{S} to $X\tilde{X}$.

Considering the OLSP having the bino (singlino) component with a fraction $c_{\tilde{B}}$ ($c_{\tilde{S}}$), we get the ratio between two decay modes as

$$\frac{c_{\tilde{B}}^2 \Gamma(\tilde{B} \rightarrow \phi\tilde{\phi})}{c_{\tilde{S}}^2 \Gamma(\tilde{S} \rightarrow X\tilde{X})} \approx 5 \times 10^{-4} \left(\frac{c_{\tilde{B}}}{c_{\tilde{S}}} \right)^2 \left(\frac{0.1}{\lambda_{\Psi}^2} \right) \left(\frac{\theta}{10^{-6}} \right)^2 \left(\frac{m_{\psi}}{700 \text{ GeV}} \right)^2 \left(\frac{200 \text{ GeV}}{m_{\tilde{\chi}_1^0}} \right)^2, \quad (5.4)$$

where we have used Eq. (4.3) and assumed $m_{\tilde{\psi}_1} \approx m_{\psi}$ for simplicity. Thus, we can conclude that χ_1^0 mostly decays to a hidden gauge boson and gaugino $X\tilde{X}$ in a reasonable choice of the parameter space. From the above calculations, the decay length of χ_1^0 is determined to be

$$l_{\chi_1^0 \rightarrow X\tilde{X}} \approx \left(\frac{0.1}{c_{\tilde{S}}} \right)^2 \left(\frac{0.1}{\lambda_{\Psi}^2} \right) \left(\frac{200 \text{ GeV}}{m_{\tilde{\chi}_1^0}} \right)^3 \times 10^{-3} \text{ cm} \quad (5.5)$$

ensuring that the OLSP decays well inside a detector. The decay-produced hidden gauge boson X decays back to the Standard Model fermion pair $f\bar{f}$ via the interaction (3.5), and the corresponding decay length is

$$l_{X \rightarrow f\bar{f}} \approx \left(\frac{1}{Q_f} \right)^2 \left(\frac{10^{-6}}{\theta} \right)^2 \left(\frac{0.4 \text{ GeV}}{m_X} \right) \times 25 \text{ cm}. \quad (5.6)$$

As a result, we will see a signal of energetic lepton pairs plus missing energy with a displacement vertex of $\mathcal{O}(10)$ cm as \tilde{X} can either be the LSP in the hidden sector or decay to a hidden sector higgs and higgsino.

Of course, this conclusion is valid only if the conventional decay channel of the OLSP to the gravitino $\psi_{3/2}$ is not too much more efficient than the above process. In GMSB models, supersymmetry breaking is driven by a hidden strong dynamics which is supposed to generate supersymmetry breaking F-term with $\sqrt{F} \gtrsim 100 \text{ TeV}$ [47]. Then the OLSP decay length for the process $\chi_1^0 \rightarrow \gamma\psi_{3/2}$ is

$$l_{\chi_1^0 \rightarrow \gamma\psi_{3/2}} \approx \left(\frac{\sqrt{F}}{10^5 \text{ GeV}} \right)^4 \left(\frac{200 \text{ GeV}}{m_{\tilde{\chi}_1^0}} \right)^5 \times 3 \times 10^{-4} \text{ cm}. \quad (5.7)$$

Remarkably, this number is comparable to (5.5), and there may be a chance to confirm both the GMSB mechanism and the presence of sub-GeV hidden $U(1)$ by observing both signals for (5.5) and (5.7).

6. Conclusion

The presence of TeV dark matter associated with a hidden $U(1)_X$ gauge symmetry broken below the GeV scale has been motivated by the recent results from PAMELA and ATIC. Elaborating this idea in the framework of gauge mediated supersymmetry breaking, we obtain some interesting constraints and prospects of the scenario.

Explaining the heaviness of dark matter in relation to the resolution of the μ and $B\mu$ problem of GMSB models, it follows that the vector-like scalar particle charged under $U(1)_X$ becomes a good dark matter candidate for the gauge coupling $\alpha_X \sim \alpha$ and the dark matter mass $\sim \text{TeV}$. The other ‘hidden’ particles, namely the $U(1)_X$ gauge boson and gaugino, higgs boson and higgsino, obtain masses below the GeV scale through a radiative mechanism with properly chosen particle contents and Yukawa couplings among them. The hidden sector communicates with the visible (Standard Model) sector either by the Yukawa terms generating the Higgsino and dark matter masses or by the kinetic mixing between $U(1)_X$ and $U(1)_Y$. It turns out that the kinetic mixing parameter θ receives a strong upper limit $\theta \lesssim 10^{-6}(m_X/0.4 \text{ GeV})^2$ coming from the experimental data on direct detection of dark matter.

In this scenario, positive signals for direct dark matter detection in future experiments may arise either from the vector interaction controlled by θ or from the scalar interaction exchanging the Higgs boson. Another interesting consequence for the LHC experiment is that the ordinary LSP decay leaves quite distinctive signals of missing energy and energetic lepton pairs with invariant mass below GeV and decay gaps larger than about 10 cm. Furthermore, the rates for this decay and the usual decay to photon and gravitino, a characteristic of GMSB models, are found to be comparable in typical parameter range of the model. Thus, the scenario of the sub-GeV $U(1)_X$ sector in GMSB models may be tested at the LHC by observing both signatures of lepton pairs plus missing energy and photons plus missing energy.

However, we find that the boost factor for the galactic dark matter annihilation required by the PAMELA and ATIC data can not be obtained solely by the Sommerfeld effect in our scenario. Typical Sommerfeld enhancement factor is in the range of 40 – 60 for the dark matter masses of 600 – 1000 GeV. Thus, we may have to invoke additional sources of the boost factor like the clumpy distribution of dark matter.

References

- [1] O. Adriani *et al.*, arXiv:0810.4995 [astro-ph]; O. Adriani *et al.*, arXiv:0810.4994 [astro-ph].

- [2] I. V. Moskalenko and A. W. Strong, *Astrophys. J.* **493**, 694 (1998)
[arXiv:astro-ph/9710124].
- [3] S. W. Barwick *et al.* [HEAT Collaboration], *Astrophys. J.* **482**, L191 (1997)
[arXiv:astro-ph/9703192]; J. J. Beatty *et al.*, *Phys. Rev. Lett.* **93** (2004) 241102
[arXiv:astro-ph/0412230].
- [4] M. Aguilar *et al.* [AMS-01 Collaboration], *Phys. Lett. B* **646**, 145 (2007)
[arXiv:astro-ph/0703154].
- [5] S. Torii *et al.*, arXiv:0809.0760 [astro-ph].
- [6] J. Chang *et al.* [ATIC collaboration], *Nature* **456**, 362 (2008).
- [7] D. Hooper, P. Blasi and P. D. Serpico, arXiv:0810.1527 [astro-ph].
- [8] H. Yuksel, M. D. Kistler and T. Stanev, arXiv:0810.2784 [astro-ph].
- [9] J. Hall and D. Hooper, arXiv:0811.3362 [astro-ph].
- [10] J. Lavalle, Q. Yuan, D. Maurin and X. J. Bi, arXiv:0709.3634 [astro-ph].
- [11] F. Donato, D. Maurin, P. Brun, T. Delahaye and P. Salati, arXiv:0810.5292
[astro-ph].
- [12] P. Grajek, G. Kane, D. J. Phalen, A. Pierce and S. Watson, arXiv:0807.1508
[hep-ph].
- [13] L. Bergstrom, T. Bringmann and J. Edsjo, arXiv:0808.3725 [astro-ph].
- [14] M. Cirelli and A. Strumia, arXiv:0808.3867 [astro-ph].
- [15] V. Barger, W. Y. Keung, D. Marfatia and G. Shaughnessy, arXiv:0809.0162 [hep-ph].
- [16] C. R. Chen, F. Takahashi and T. T. Yanagida, arXiv:0809.0792 [hep-ph].
- [17] I. Cholis, L. Goodenough, D. Hooper, M. Simet and N. Weiner, arXiv:0809.1683
[hep-ph].
- [18] M. Cirelli, M. Kadastik, M. Raidal and A. Strumia, arXiv:0809.2409 [hep-ph].
- [19] J. H. Huh, J. E. Kim and B. Kyae, arXiv:0809.2601 [hep-ph].
- [20] N. Arkani-Hamed, D. P. Finkbeiner, T. Slatyer and N. Weiner, arXiv:0810.0713
[hep-ph].
- [21] M. Pospelov and A. Ritz, arXiv:0810.1502 [hep-ph].
- [22] M. Fairbairn and J. Zupan, arXiv:0810.4147 [hep-ph].
- [23] A. E. Nelson and C. Spitzer, arXiv:0810.5167 [hep-ph].

- [24] I. Cholis, D. P. Finkbeiner, L. Goodenough and N. Weiner, arXiv:0810.5344 [astro-ph].
- [25] Y. Nomura and J. Thaler, arXiv:0810.5397 [hep-ph].
- [26] R. Harnik and G. D. Kribs, arXiv:0810.5557 [hep-ph].
- [27] D. Feldman, Z. Liu and P. Nath, arXiv:0810.5762 [hep-ph].
- [28] P. f. Yin, Q. Yuan, J. Liu, J. Zhang, X. j. Bi and S. h. Zhu, arXiv:0811.0176 [hep-ph].
- [29] K. Ishiwata, S. Matsumoto and T. Moroi, arXiv:0811.0250 [hep-ph].
- [30] Y. Bai and Z. Han, arXiv:0811.0387 [hep-ph].
- [31] P. J. Fox and E. Poppitz, arXiv:0811.0399 [hep-ph].
- [32] C. R. Chen, F. Takahashi and T. T. Yanagida, arXiv:0811.0477 [hep-ph].
- [33] A. Ibarra and D. Tran, arXiv:0811.1555 [hep-ph].
- [34] S. Baek and P. Ko, arXiv:0811.1646 [hep-ph].
- [35] I. Cholis, G. Dobler, D. P. Finkbeiner, L. Goodenough and N. Weiner, arXiv:0811.3641 [astro-ph].
- [36] E. Nardi, F. Sannino and A. Strumia, arXiv:0811.4153 [hep-ph].
- [37] K. M. Zurek, arXiv:0811.4429 [hep-ph].
- [38] M. Pospelov, A. Ritz and M. B. Voloshin, Phys. Lett. B **662**, 53 (2008) [arXiv:0711.4866 [hep-ph]].
- [39] N. Arkani-Hamed and N. Weiner, arXiv:0810.0714 [hep-ph].
- [40] H. Baer, K. m. Cheung and J. F. Gunion, Phys. Rev. D **59**, 075002 (1999) [arXiv:hep-ph/9806361].
- [41] J. Hisano, S. Matsumoto and M. M. Nojiri, Phys. Rev. D **67**, 075014 (2003) [arXiv:hep-ph/0212022]; J. Hisano, S. Matsumoto and M. M. Nojiri, Phys. Rev. Lett. **92**, 031303 (2004) [arXiv:hep-ph/0307216]; J. Hisano, S. Matsumoto, M. M. Nojiri and O. Saito, Phys. Rev. D **71**, 015007 (2005) [arXiv:hep-ph/0407168]; J. Hisano, S. Matsumoto, M. M. Nojiri and O. Saito, Phys. Rev. D **71**, 063528 (2005) [arXiv:hep-ph/0412403]; J. Hisano, S. Matsumoto, O. Saito and M. Senami, Phys. Rev. D **73**, 055004 (2006) [arXiv:hep-ph/0511118]; J. Hisano, S. Matsumoto, M. Nagai, O. Saito and M. Senami, Phys. Lett. B **646**, 34 (2007) [arXiv:hep-ph/0610249].
- [42] S. Profumo, Phys. Rev. D **72**, 103521 (2005) [arXiv:astro-ph/0508628].
- [43] M. Cirelli, A. Strumia and M. Tamburini, Nucl. Phys. B **787**, 152 (2007) [arXiv:0706.4071 [hep-ph]].

- [44] J. March-Russell, S. M. West, D. Cumberbatch and D. Hooper, JHEP **0807**, 058 (2008) [arXiv:0801.3440 [hep-ph]].
- [45] L. B. Okun, Sov. Phys. JETP **56**, 502 (1982) [Zh. Eksp. Teor. Fiz. **83**, 892 (1982)]; B. Holdom, Phys. Lett. B **166**, 196 (1986).
- [46] J. H. Huh, J. E. Kim, J. C. Park and S. C. Park, Phys. Rev. D **77**, 123503 (2008) [arXiv:0711.3528 [astro-ph]].
- [47] M. Dine and A. E. Nelson, Phys. Rev. D **48**, 1277 (1993) [arXiv:hep-ph/9303230]; M. Dine, A. E. Nelson and Y. Shirman, Phys. Rev. D **51**, 1362 (1995) [arXiv:hep-ph/9408384]; M. Dine, A. E. Nelson, Y. Nir and Y. Shirman, Phys. Rev. D **53**, 2658 (1996) [arXiv:hep-ph/9507378].
- [48] K. Agashe and M. Graesser, Nucl. Phys. B **507**, 3 (1997) [arXiv:hep-ph/9704206]; A. de Gouvea, A. Friedland and H. Murayama, Phys. Rev. D **57**, 5676 (1998) [arXiv:hep-ph/9711264].
- [49] D. Feldman, Z. Liu and P. Nath, Phys. Rev. D **75**, 115001 (2007) [arXiv:hep-ph/0702123].
- [50] A. Ibarra, A. Ringwald and C. Weniger, arXiv:0809.3196 [hep-ph].
- [51] G. Bertone, D. Hooper and J. Silk, Phys. Rept. **405**, 279 (2005) [arXiv:hep-ph/0404175].
- [52] E. Komatsu *et al.* [WMAP Collaboration], arXiv:0803.0547 [astro-ph].
- [53] G. Jungman, M. Kamionkowski and K. Griest, Phys. Rept. **267**, 195 (1996) [arXiv:hep-ph/9506380].
- [54] C. P. Burgess, M. Pospelov and T. ter Veldhuis, Nucl. Phys. B **619**, 709 (2001) [arXiv:hep-ph/0011335].
- [55] D. P. Finkbeiner, T. Slatyer and N. Weiner, Phys. Rev. D **78**, 116006 (2008) [arXiv:0810.0722 [hep-ph]].
- [56] H. S. Lee. *et al.* [KIMS Collaboration], Phys. Rev. Lett. **99**, 091301 (2007) [arXiv:0704.0423 [astro-ph]].
- [57] Z. Ahmed *et al.* [CDMS Collaboration], arXiv:0802.3530 [astro-ph].
- [58] D. Tucker-Smith and N. Weiner, Phys. Rev. D **64**, 043502 (2001) [arXiv:hep-ph/0101138].
- [59] P. Fayet, Phys. Rev. D **75**, 115017 (2007) [arXiv:hep-ph/0702176].